

Presented at the Heavy Ion Fusion
Workshop, Argonne National Laboratory,
Argonne, Illinois, September 19-26, 1978

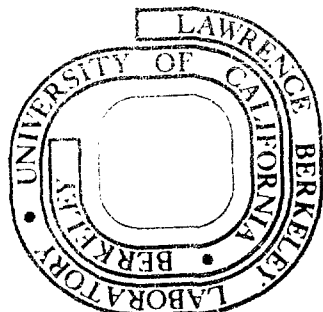
LBL-8494

STATUS REPORT ON THE
LAWRENCE BERKELEY LABORATORY
HEAVY ION FUSION PROGRAM

D. Keefe, A. Fallens, E. Hoyer, L. J. Laslett, S. Abbott,
W. Chupp, D. Clark, C. Kim, R. Richter, S. Rosenblum, J. Shiloh,
J. Staples, E. Zajec, W. Herrmannsfeldt

November 1978

Prepared for the U. S. Department of Energy
under Contract W-7405-ENG-48



MASTER

The essence of our design procedure is to pick a specific total beam charge $[I_T]$, one value in a sequence, and examine the differential cost, ΔC , required to add an increment of voltage $\Delta V = 1$ MV to the beam at each voltage point, V , along the accelerator. In general, there is a minimum value of $\Delta C/\Delta V$ at each voltage point, V , which in turn determines the exact design for the accelerating modules, pulsers and magnets at that point; if one seeks for example, a minimum-cost accelerator, the entire design is determined and the cost -- except for the injector and final beam manipulation sections -- is given by

$$\left[C_{\min} \right]_{[I_T]} = \left[\int_{V_{inj}}^{V_f} \left(\frac{\Delta C}{\Delta V} \right)_{\min} dV \right]_{[I_T]} \quad (1)$$

In most cases some departure from the minimum-cost design, particularly at the higher voltage points, is desirable for electrical efficiency reasons and for meeting the final longitudinal requirements. Thus it is important to have detailed information of the nature of the $\Delta C/\Delta V$ variation, i.e., whether it is a broad or narrow stationary minimum or if it is a non-stationary minimum arising from a constraint. See Fig. 1 for an example $\Delta C/\Delta V$ curve.

That, in principle, a stationary minimum for $\Delta C/\Delta V$ exists can be illustrated as follows. The volt-second requirements for the cores to add 1 MV is

$$\text{Volt-Secs} = 10^6 \int_{I_T} = 10^6 \frac{[I_T]}{I} \cdot (I)^{-1} \quad (2)$$

Thus lower core and pulser costs can be achieved by arranging for the highest beam-current; this requires a high density of transport magnets (occupancy fraction, η , approaching unity). The current I attains its maximum value as $\eta \rightarrow 1$ but this leaves no space at all for the accelerating cores and the cost to add 1 MV tends to infinity. Conversely, the cost of the magnet system can be lower by operating at low beam-current (i.e., $\eta \rightarrow 0$) which in turn, from Eqn. 2, implies increased volt-seconds of core and likewise cost. Between these extremes there is an appropriate partition between the space occupied by accelerating cores which leads to a minimum cost. While a stationary minimum exists in principle, there are cases at the low-current end of the accelerator where the stationary point is not accessible in practice -- usually because of the need to restrict the quadrupole pole-tip field to a manageable value (≈ 4 T).

In December 1977, a first Reference Conceptual Design, called IL 4/26, was described for a 1 MJ, 156 TW driver using U^{+4} ions accelerated to 26 GeV (i.e., $V_f = 6.5$ GV).⁽²⁾ While we were aware at that time of the general design criteria described above, the detailed cost data required for evaluating cost-minima were not yet in hand then and the choices of induction-core and magnet configurations at various points along the accelerator were simply a matter of educated guessing. A block-diagram showing some of the parameters in that design is given in Figure 2. The injector (which included the stripping section) provided $[I_T] = 755 \mu\text{C}$ and was based upon three stages of pulsed drift-tube acceleration⁽³⁾ with solenoid focussing. An appropriate bunching section was designed for the latter part of the accelerator after which the beam was allowed to become large transversely and split with a four-way septum magnet to enter the final four transport lines leading to the target chamber.

The points to be emphasized here that influence the interpretation of the partially-complete results that follow are:

- In Reference Design IL 4/26 the injector cost was about 10% of the accelerator system, and the final beam transport also represented about 10% of the cost.
- Because 80% of the cost was identified (for that case) to reside in the induction linac part from the injection voltage (50 MV) to the final voltage, $V_f = 6.5$ GeV, we decided to concentrate our efforts on refining the design procedure for this major-cost part of the system, and these are the results that are discussed below.
- We believe that the costs of the final transport and focussing systems for most of the parameter ranges to be discussed will indeed be of the order of 10% of the overall system cost, or possibly less.
- We are uncomfortable at this time about stating the scaling law for the injector cost as a function of the beam-charge $[I\tau]$ delivered. It is certainly less than linear with total charge, since at worst several injectors may always be paralleled in a tree configuration. Undoubtedly the injector cost will increase with increasing $[I\tau]$ while the induction linac cost will decrease (see below) for reasonable assumptions about the beam emittance. Thus the "10% injector-cost" rule will be violated if we wish to scale too far away from Reference Design IL 4/26, and as yet we cannot furnish a reliable estimate of by how much. The high current injector design presents a fascinating design question, and there is room and need for innovation. Several interesting ideas need pursuing, but up to this date - apart from examining some designs in the spirit of existence proofs - we have felt it more important first to address in a proper way the cost-dominating section of the system.
- Results for costs for the induction linac section given below can be referred to as "80% of cost" values but with the caveat that if one strays too far from the IL 4/26 case of $[I\tau] = 155 \mu\text{C}$, the 80% figure becomes unreliable. We feel now that a preferred reference example would be IL 4/19 with $[I\tau] = 210 \mu\text{C}$ and that more study of the injector is needed before cases with much larger $[I\tau]$ values can be reliably costed. (4)

2. Cost Procedure

Up to this point we have simplified the problem in studying the "80% - cost figure" by assuming

- (i) A suitable injector at $V_{inj} = 50$ MV is available (this has been established in detail only for the Reference Design IL 4/26).
- (ii) The final rapid-buncher section costs about the same as if it were composed of a pure accelerating section with modest bunching. (In Reference Design IL 4/26 the cost differential was small).

More work is needed on both of these topics before they can be incorporated in detail into a comprehensive cost-estimating program.

To address the main part of the Induction Linac system, viz. the "80% part", a computer program (LIACEP) has been developed to sort through the possible engineering options at each voltage point, V , along the machine and to generate the desired cost and design information.

We start by specifying an ion species with atomic weight, A , and charge state, q , (so far only Uranium with charge states 1, 2, and 4, and Cs with charge state 1, have been studied). Next, an electrical beam charge $[I_{\text{e}}]$ is specified with a sequence to be explored -- 30 μC , 60 μC , 90 μC ..., etc., ... up to 1000 μC . Then at any voltage point, V , along the accelerator the cost consequences of adding a further 1 MV are examined. The independent variable is chosen to be the current, I , with the magnet occupancy factor, r_1 , for a symmetrical FODO lattice, as a separately set and varied parameter (e.g., $r_1 = .5, .33, .17, .10, .05$, etc.). In this way a set of curves for each value of r_1 can be generated to display differential cost versus current and so to arrive at a minimum or indicate the cost/benefit ratio of departing from the minimum (see Fig. 1).

At this point we have to identify three distinct classes of information which are key ingredients of the optimization process:

- (1) Engineering Design Options and Constraints
- (2) Cost data base which can affect the trade-off among design choices
- (3) Physics assumptions about (i) the desirable beam emittance determined by the pellet and transport requirements, or the realizable beam emittance set by the source performance, and; (ii) the transverse space charge limiting current.

These input classes are discussed in sequence below. At this time the greatest cost uncertainties seem to arise from the consequences of the physics assumptions.

(1) Essential to this costing routine is the spectrum of engineering options that are examined in the process. To date we have chosen to input the engineering possibilities and constraints listed below. A few of the options, identified by the asterisk, have not yet been exercised in the program (which is still under development):

- A: Accelerating module design based upon an economic choice between iron or ferrite
- A: Accelerating module design based upon an economic choice between amorphous ferromagnetics or ferrite⁽⁵⁾
- B: A module design with the oil-vacuum interface insulator near the inner radius of the cores (Fig. 3)
- B: A module design with the insulator near the outer radius of the cores (Fig. 4)
- B: A module design wherein the transport magnets can be re-entrant within the pulsed cores (most appropriate for low- β section)

- * B: A module design with radial sub-division of the cores⁽⁶⁾
- * C: Conventional-conductor/iron quadrupole transport magnets (appropriate for test facility but probably not for power-plant)
 - C: Superconducting quadrupole magnets
 - D: Constraint that the quadrupole "pole-tip" field does not exceed 4T
 - D: Constraint that the quadrupole bore-radius to length ratio never exceeds 0.25.
 - D: Constraint that the electrical stress on the insulator never exceeds 10 kV per cm for pulse duration greater than 1 μ sec and 10-40 kV per cm for pulse durations of less than 1 μ sec.
 - D: Constraint that the "longitudinal space-charge factor" (LSCF) never exceeds 0.1. The LSCF is defined as the ratio of the extra gradient needed to hold together the ends of a beam bunch with 10% tapered ends to the average accelerating gradient. This constraint implies at most an extra 1-2% of overall core volt-seconds in the accelerator if separate longitudinal focussing modules are used.
 - D: Constraints on the maximum "reasonable" radius of a core and on the maximum weight of an assembled module.
 - D: Constraint that the maximum beam-pipe bore radius not exceed 0.2 m.

(2) The cost input data are of such complexity that they cannot be discussed in detail in this report. Briefly, their breakdown falls under the following headings:

A. Technical Components

1. Accelerating Modules (cores, insulators, structures, etc.)
2. Pulsers
3. Vacuum System
4. Support and Alignment
5. Control Room
6. Computer System
7. Beam monitoring and control
8. Quadrupoles, refrigeration and cryogenic distribution, power supplies, testing, control, support and alignment.

B. Conventional Facilities

1. Site Work
2. Accelerator Housing
3. Control Room Building

4. Mechanical Facilities
5. Electrical Facilities
6. Safety

Details of the unit costs based upon manufacturers' quotes, and the interpolation or extrapolation formulas based upon projects completed or under construction are documented in internal LBL engineering notes by E. Hoyer. An obvious advantage of having the program, LIACEP, to sort through many cases is that by varying the input cost data we can quickly identify those items or design features to which the overall costs are most sensitive

(3) Until adequate experiments can be carried out for high current heavy ion beams on achievable beam brightness and on the details of the transverse space-charge limit we shall continue to have uncertainties in specifying these quantities precisely. These uncertainties span actually a rather narrow range but unfortunately can lead to significant cost effects. The first of these arises from the fact that in the final focussing lens the third-order geometric aberrations impose a condition that the entering beam (or beamlet) have an upper limit on emittance. From the work of Garren⁽⁸⁾ and Neuffer⁽⁹⁾ we have derived the following approximate expression for this emittance limit in a single plane (x, for example):

$$\epsilon_N^L \lesssim 0.12 \text{ Br } r_s^{4/3} \quad (3)$$

where the superscript, L, refers to the doublet lens, the subscript, N, indicates normalized emittance, and r_s is the target spot radius. If we denote by ϵ_N^T the total normalized emittance of the beam transported through the accelerator then the number of final separate beamlets, N_b , required to meet the target needs can be expressed as

$$N_b \geq \frac{(\epsilon_N^T)_{\text{HORIZ}} (\epsilon_N^T)_{\text{VERT}}}{(\epsilon_N^L)_{\text{HORIZ}} (\epsilon_N^L)_{\text{VERT}}} = \frac{2}{3} \left(\frac{\epsilon_N^T}{\epsilon_N^L} \right)^2 \quad (4)$$

where the factor 2/3 arises from the fact that in the y-plane the emittance can be some 50% larger than the x-plane emittance limit given by Eqn. (3); this comes about because of the inherent x-y asymmetry of a doublet lens.

An example of a four-beamlet splitter using current-sheet septum splitting magnets and quadrupoles is shown in Fig. 5. This represents one half of an "eight-beamlet" system for pellet irradiation, i.e., two clusters of four beamlets from opposite directions. When one examines the engineering details of arranging for a large number of beamlets in a cluster then it appears that the complexity becomes formidable for N_b much in excess of 20.

These considerations thus impose a constraint on the total beam emittance, ϵ_N^T , that can be tolerated in the accelerator and this probably should not exceed 3×10^{-5} rad for the reference 1 MJ design. The studies show that the capital cost decreases and the electrical efficiency increases if a higher value of emittance can be tolerated; this comes about because the space charge

limited current is proportional to $(\epsilon_N^T)^{2/3}$. This sensitivity of cost and efficiency to the space-charge limited current seems a general feature and it becomes important to have a good understanding of what betatron tune depression can be safely tolerated in the transport system. Extensive studies of this question have been carried out by Laslett using computational techniques for a Kapchinskij-Vladimirskij distribution⁽¹¹⁾ and by Haber using numerical simulation codes.⁽¹²⁾ Conclusions have varied somewhat from time to time and a convincing final result is not yet available. Early LIACEP program runs used a tune depression $\sigma_0 \rightarrow \sigma$ of $90^\circ \rightarrow 36^\circ$, later this was revised to $90^\circ \rightarrow 57.5^\circ$ and still later to $60^\circ \rightarrow 24^\circ$. The non K-V case results by Haber⁽¹³⁾ suggest that a tune depression $90^\circ \rightarrow 30^\circ$ may perhaps be tolerable, but no cost study has been made for this case. Such uncertainties in the tune-depression specification are reflected in cost uncertainties of as much as 20%.

The LIACEP program procedure for a particular choice of tune-depression is to pre-set the magnet occupancy factor, η , and calculate magnet length, period length, and magnet pole tip field for a variety of beam currents, and later to cycle through several values of η . Thus in any instance the magnet parameters and the available space for the accelerating modules is derived and the appropriate engineering solutions described earlier can be examined.

3. Results

It must be emphasized that these "80% cost" studies are useful as a design guide and as a tool for identifying the cost sensitivity to any of the input assumptions and engineering options and costs. Thus the absolute value of the cost figures should be treated with considerable caution and attention focussed on the trends suggested by the data; in our view, reliable costs can be derived only when a particular case is settled upon and an ab initio design carried through in detail for that case. The sample results given here reflect work-in-progress, and inconsistencies in assumptions will be noticed. Fig. 6 shows example results for minimum "80%-cost" designs as a function of charge-state for uranium and an example point for Cs^{+1} . The interesting result is that the variation is not large but higher charge states are favored on cost grounds by perhaps 25%. There are physics arguments favoring the lower charge states which correspond to lower kinetic-energy (shorter range) examples.

These examples used a tune depression $90^\circ \rightarrow 57.5^\circ$ and an emittance $\epsilon_N^T = 2 \times 10^{-5}$ rad-m.

Fig. 7 shows costs for U^{+4} (again for the same tune-shift) if the emittance can be permitted to be as high as 4×10^{-5} rad-m, and constant at that value independent of the beam charge $[I_T]$. The minimum for most energies seems broad and in the range $[I_T] = 200 - 500 \mu\text{C}$.

Fig. 8 shows costs for U^{+4} with different assumptions for tune-shift ($60^\circ \rightarrow 24^\circ$) and emittance. The normalized emittance is assumed to be 3×10^{-5} rad m up to $[I_T] = 210 \mu\text{C}$ and to scale as $[I_T]^{1/2}$ beyond that point. If the increased beam charge is achieved by increasing the area of the ion source then this square-root law would arise naturally. The increase of emittance for higher beam charge does not lead to difficulties in the final focus since the target spot radius can also be larger. Note that the curves for fixed joules tend monotonically downward towards higher beam charge; this

arises primarily from the corresponding allowed increase in emittance. It must be emphasized again, however, that the cost of the injector will increase as $[I_T]$ increases and the overall cost of the accelerator may show a stationary minimum.

Fig. 9 summarizes information for the new reference design IL4/19. Illustrated are the theoretical maximum current variation as a function of voltage along the accelerator (close-packed magnets, and tune-shift $60^\circ \times 24^\circ$), the practical maximum current set by the structure constraints discussed earlier, and the way the current would vary for an accelerator that used the minimum-cost solution at each point. Also shown are the ranges of beam-current variation allowed for costs up to 20% above minimum. The higher the current the higher will be the electrical efficiency so if the latter were to be a prime consideration for the 1 MJ driver it could pay to choose to increase the capital cost of the last part of the accelerator by some 20%.

TABLE I

Example Parameter Choices for a 1 MJ U^{+4} Driver

$[I_T]$ μC	T GeV	V GV	R g/cm ²	R _T mm	ϵ_N^T ($\times 10^5$) rad-m	ϵ_N^T ($\times 10^5$) rad-m	N _B
150	26.7	6.67	.78	1.01	.77	3	10
210	19.0	4.76	.5	1.26	.69	3	12
300	13.3	3.33	.33	1.55	.79	3.6	14
500	8.0	2.0	.17	2.16	.935	4.6	16
1000	4.0	1.0	.08	3.15	1.07	6.6	25

Table I shows a variety of parameter options for a 1 MJ driver. The first entry is close to the old Reference Case IL4/26 and the second entry corresponds to the new Reference Case IL4/19. The succeeding entries have advantages in allowing large pellet radii but realistic injector designs will have to be developed for each before they can be properly evaluated.

We wish to acknowledge the help of Mr. Victor Brady in performing much of the computational work.

References and Notes - Part I

1. D. Eccleshall and J.K. Temperly, Transfer of Energy From Charged Transmission Lines with Applications to Pulsed High-Current Accelerators, J.A.P. 49 (7), July, 1978.
2. Preliminary Cost Figures for an Induction Linac, HIF Staff, HI-FAN-54, 1977.
3. A. Faltens and D. Keefe, Particle Accelerators 8, 245 (1978).
4. LBL HIF Staff, Linear Induction Accelerator Conceptual Design, HI-FAN-58, 1978.
5. Amorphous ferromagnetic tape material is under intensive study for low-loss motors and transformers by Allied Chemical (under the trade name METGLAS), G.E., and several universities. It is made in typical thicknesses of 0.001" - 0.002" and has high resistivity. Extensive descriptions and references can be found in Amorphous Magnetism II, edited by R.A. Levy and R. Hasegawa, Plenum Press, N.Y. and London, 1977.
6. Modules with four-fold and five-fold radial sub-divisions have been studied and are in operation at NBS, see Preliminary Report of Prototype Induction Accelerator Performance, M.A. Wilson, and J.E. Leiss, N.B.S., Washington, D.C.
7. E. Hoyer, Summary of Induction Linac Cost Factors, Eng. Note M5250, (1978).
8. A. Garren, Final Focusing of the Ion Beams of a Pellet Fusion Reactor by Quadrupole Doublets, Proc. 1976 HIF Workshop, LBL-5543.
9. D. Neuffer, Geometric Aberration in Final Focusing, HI-FAN-36, (1978).
10. D. Neuffer, Unpublished, (1978).
11. L.J. Laslett, L. Smith; J. Bisognano, Computational Study of a Third-Order Instability Suggested by Computations of Dr. Haber, HI-FAN-43, (1978).
12. I. Haber and A. Maschke, Steady State Transport of High Current Beam in a Focused Channel, NRL-3787, (1978).
13. I. Haber, private communication, October, 1978.

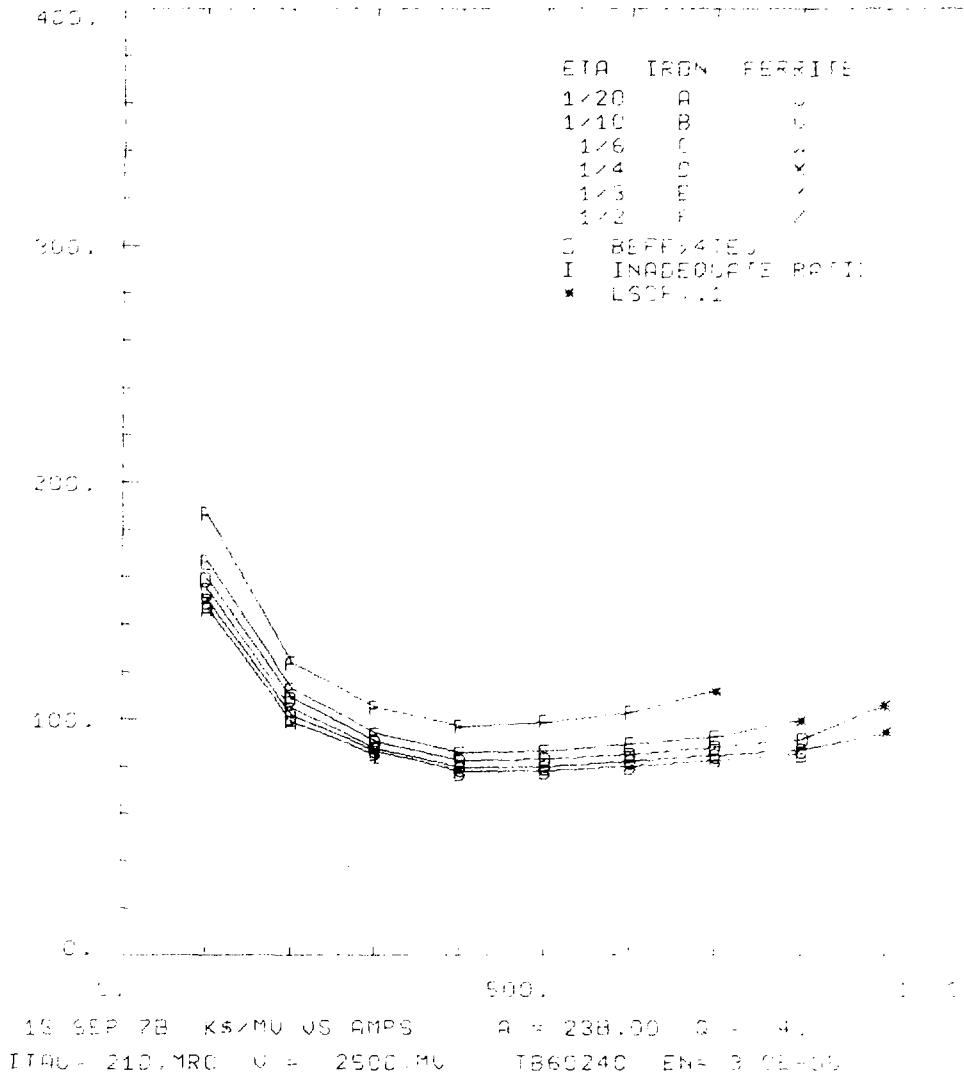
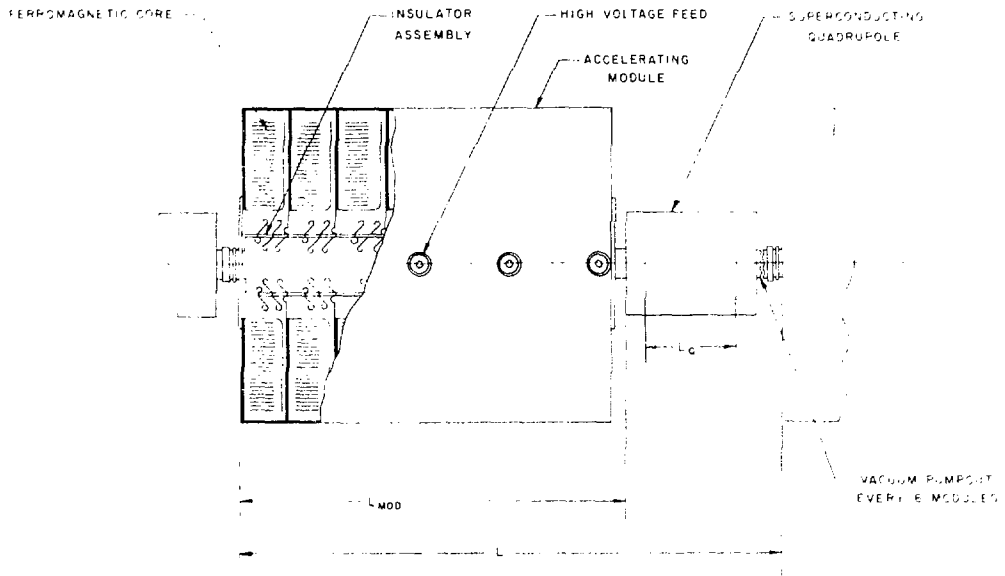


Figure 1
EXAMPLE COST CURVE



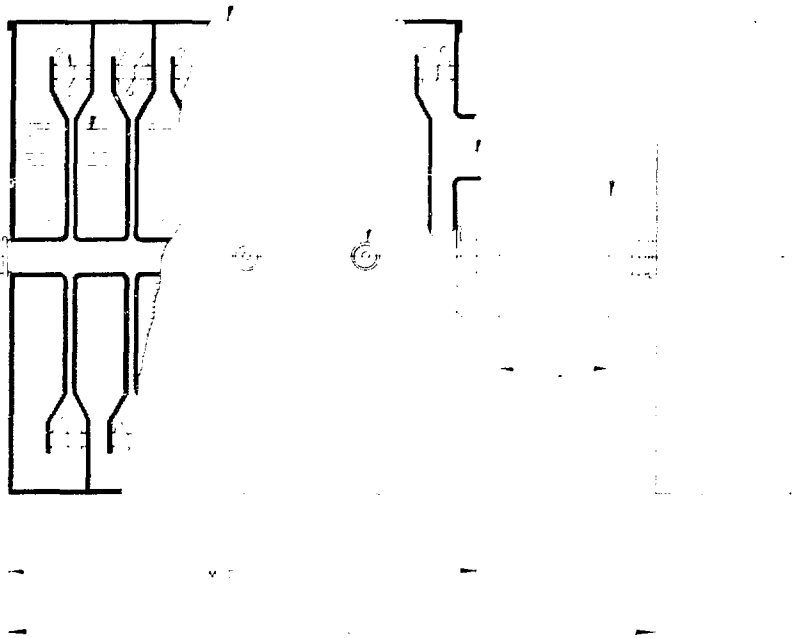
FERROMAGNETIC CORE MODULE - TYPE 2

Figure 3

XBL 789-10717

INSULATOR ASSEMBLY FERROMAGNETIC CORE HIGH VOLTAGE FEED PERTINENT QUADROPOLE

ACCELERATING MODULE VACUUM PUMP OUT



FERROMAGNETIC CORE MODULE - TYPE I

Figure 4

XBL 769-10716

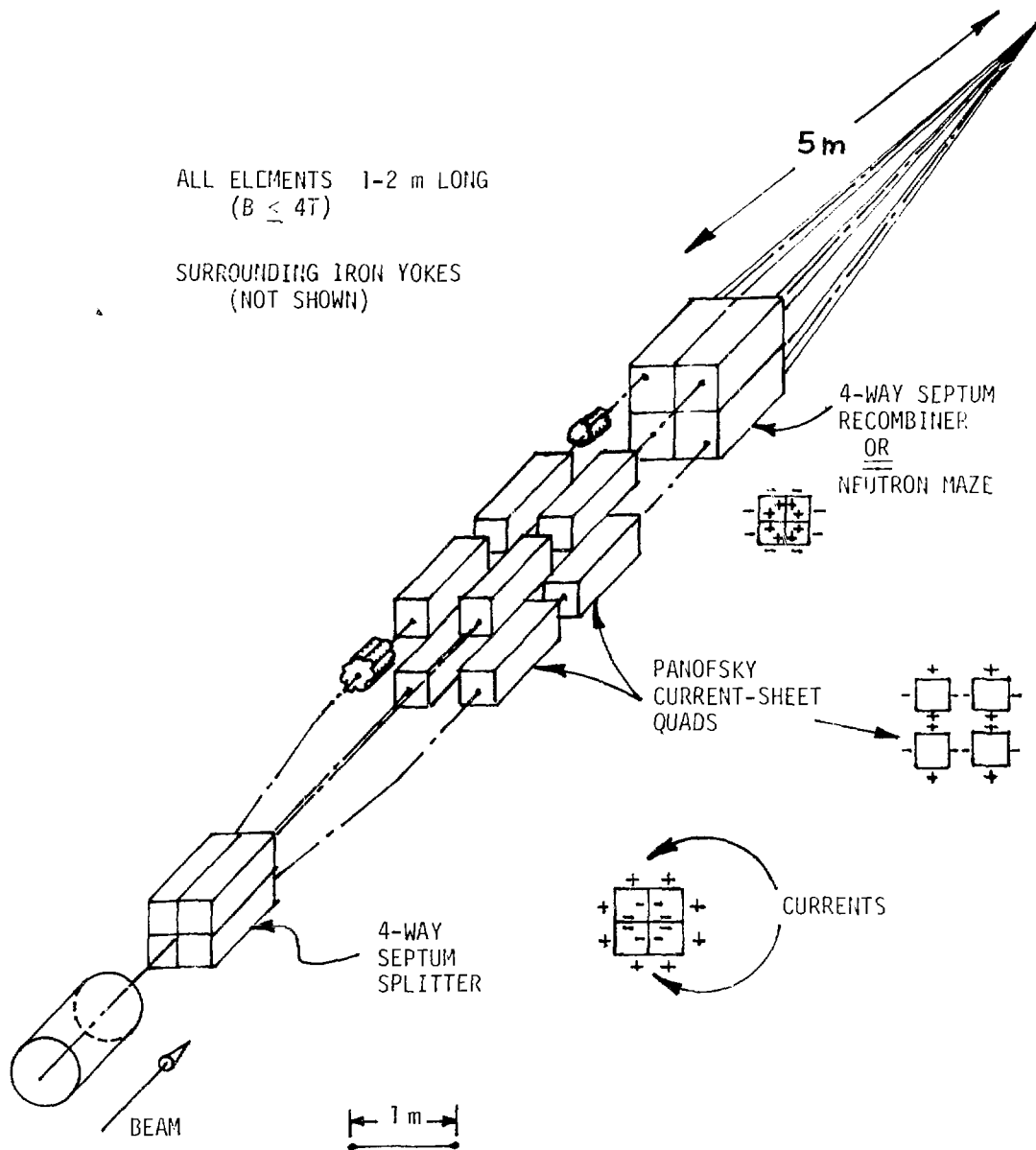


Figure 5

SCHEMATIC - 1 BEAM TO 4 BEAM SPLIT AND FOCUS

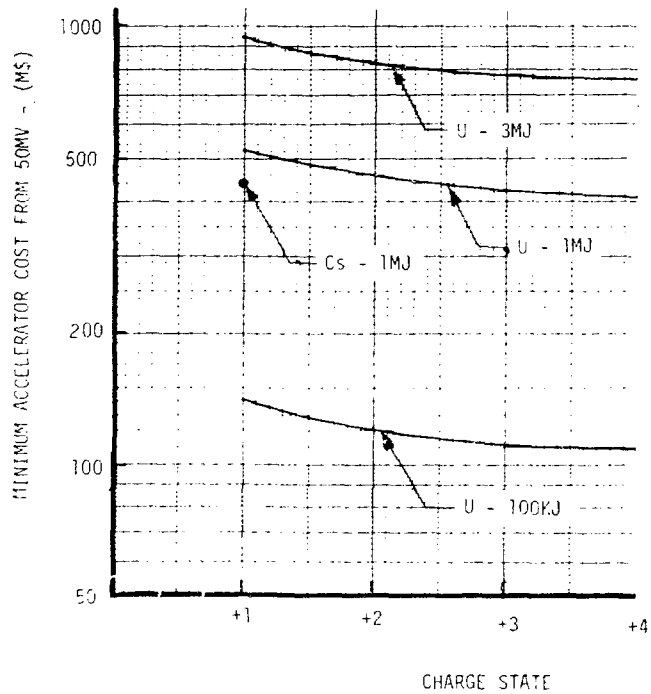


Figure 6

MINIMUM INDUCTION ACCELERATOR COST
FROM 50W USING METALLIC GLASS

CORES FOR URANIUM & CESIUM FOR

90° - 57.5° PHASE SHIFT, &

$H = 2.0 \times 10^{-5}$ M-RAD

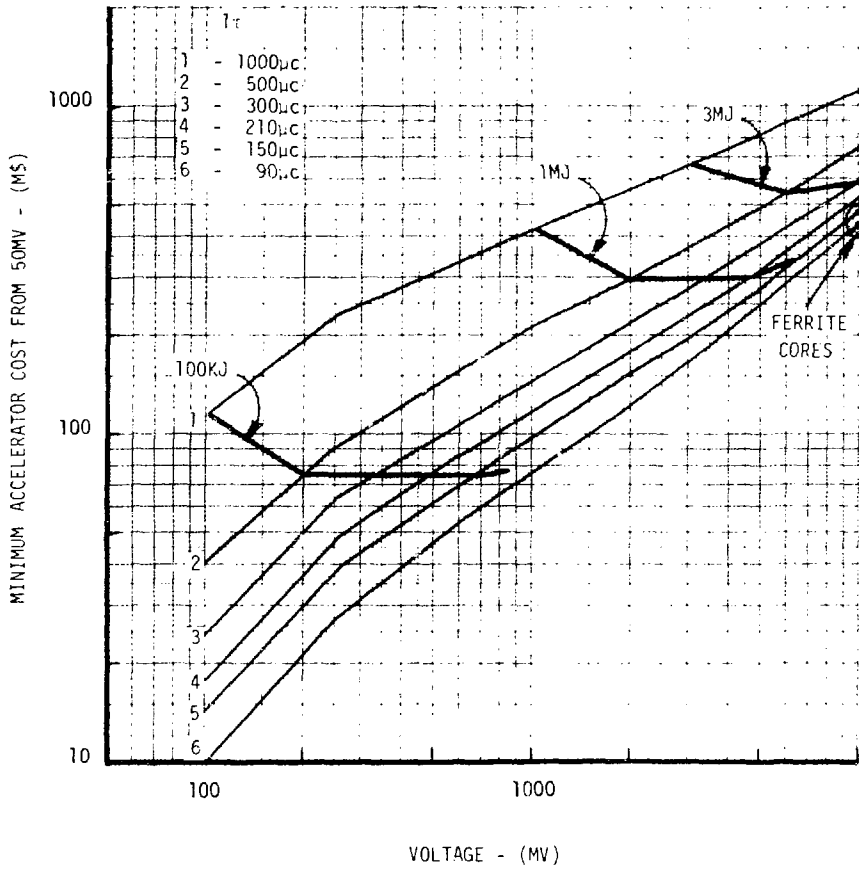


Figure 7

MINIMUM INDUCTION ACCELERATOR COST FROM 50MV USING METALLIC GLASS

U^{+4} , $90^\circ - 57.5^\circ$ PHASE SHIFT, & $E_N = 4.0 \times 10^{-5}$ M-RAD

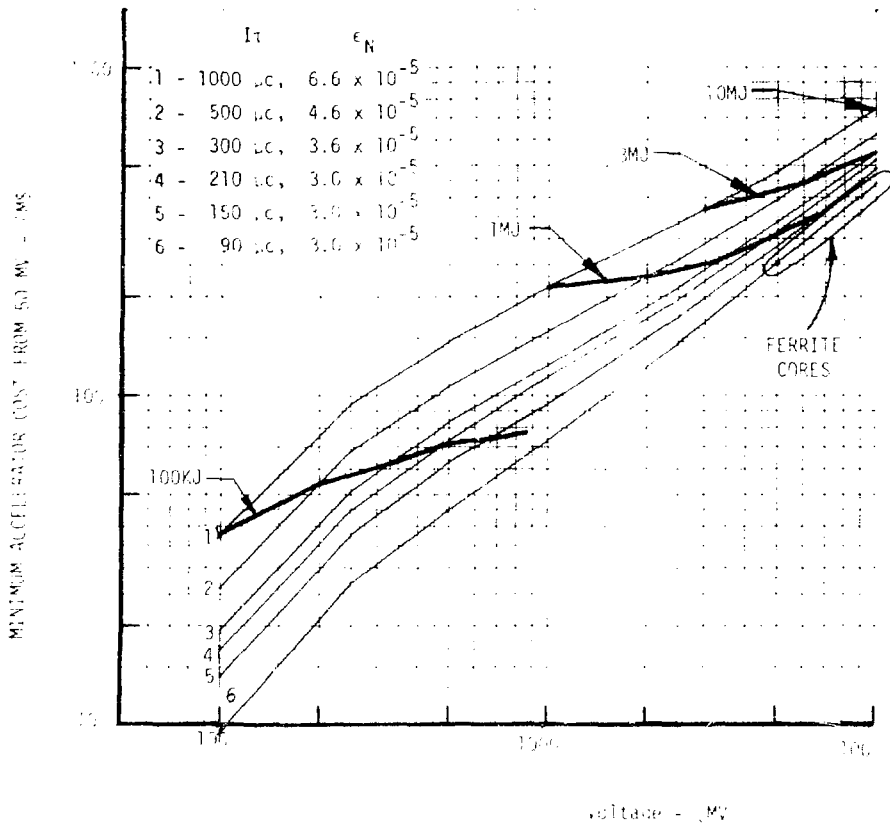


Figure 8

MINIMUM INDUCTION ACCELERATOR COST FROM 1 MW USING METALLIC GLASS
& FERRITE CORES FOR $A = 23\%$, $\alpha = +4$, $\beta = -24$ TONE SHIFT

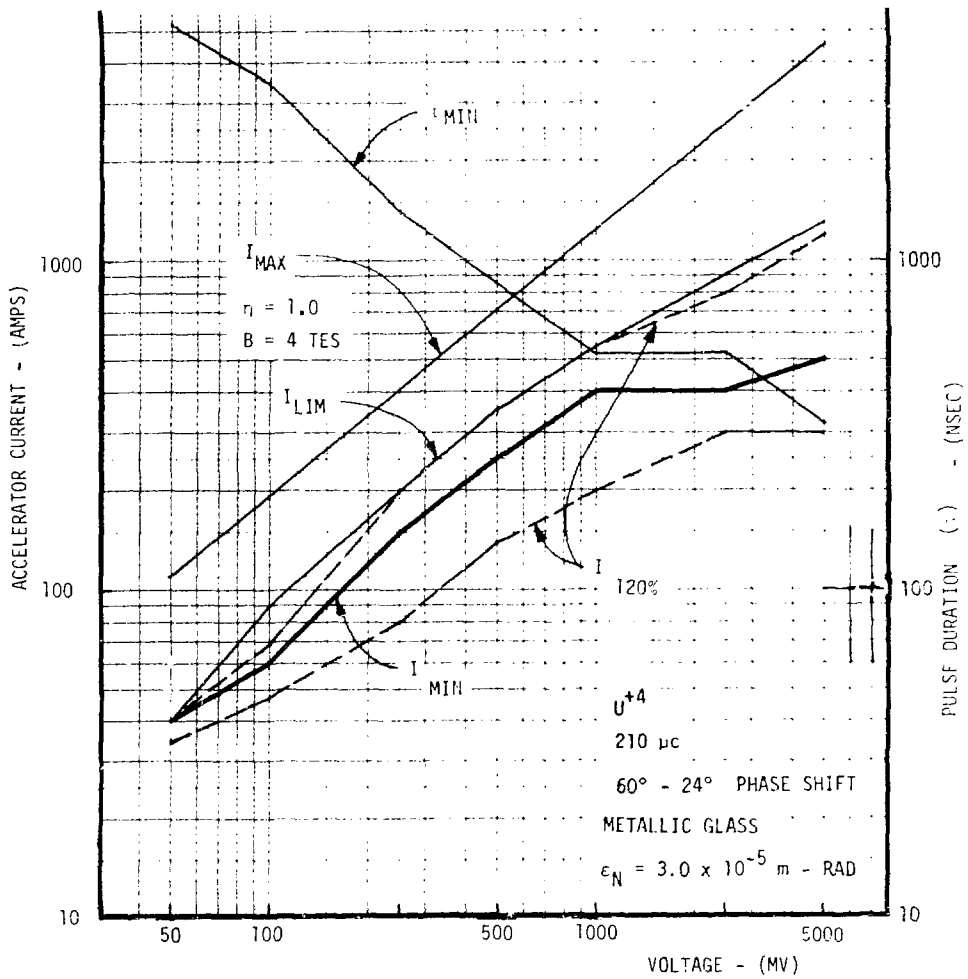


Figure 9

ACCELERATOR CURRENT AND PULSE
DURATION FOR REFERENCE I.L.
CASE 4/19 (1MJ - 100 TW)

PART II. THEORETICAL ACTIVITIES

(presented by D. Keefe)

Progress this year has been achieved in three major areas:

A. Beam Transport (J. Bisognano, I. Hofmann, L.J. Laslett, L. Smith)

Further work on instabilities of the Kapchinskij-Vladimirskij (K.V.) distribution has led to revision of the recommended choice of maximum transportable power for design purposes. A significant achievement has been the successful comparison between our theoretical results and the simulation computations by Irving Haber for a particular unstable mode; this comparison gives credence to both the theoretical and simulation work and suggests that the simulation approach can be trusted when applied to more realistic distributions, which cannot be treated analytically.

B. Final Focussing (A. Garren, D. Neuffer)

The work of A. Garren⁽¹⁾ on the parametrization of a final focusing doublet has been extended to triplets, which are more suitable in certain parameter regimes. The effect of third order geometric and fringing field aberrations in the final lens system has been explored, leading to constraints on the emittance of the individual beams approaching the target. The effect of chromatic aberrations has been studied quantitatively and appears to be somewhat more serious than indicated by the previously used rule of thumb; work has begun on the correction of these aberrations by the use of bending magnets and sextupoles upstream from the final lens system.

C. Parameter Studies (D. Judd, L. Smith)

In light of the constraints imposed by the final focusing system, the six-dimensional phase space requirements have been re-formulated and used to develop a number of r.f. linac and synchrotron scenarios. As others have found, the synchrotron schemes do not look very attractive, particularly since the trend this year has been toward lower kinetic energy and higher current, whereas the virtue of a synchrotron is rather to provide high kinetic energy at low current.

References

1. A. A. Garren, Report of Summer Study of Heavy Ions for Inertial Fusion, July 19-30, 1976, LBL-5543, p. 102.

Part III: THE EXPERIMENTAL PROGRAM ON HEAVY ION FUSION
AT LAWRENCE BERKELEY LABORATORY*

S. Abbott, W. Chupp, D. Clark, A. Faltens, E. Hoyer
D. Keefe, C. Kim, R. Richter, S. Rosenblum,
J. Shiloh, J. Staples, E. Zajec
Lawrence Berkeley Laboratory

W. Herrmannsfeldt
Stanford Linear Accelerator Center

(Presented by C. Kim)

1. Introduction

The experimental efforts at LBL have been focused on both the development of a large aperture 2 MeV, 1A Cs⁺¹ ion beam¹⁾ using contact ionization and drift tube techniques as an injector for an induction linac and, also, a 750 kV, 60 mA Xe⁺¹ ion beam²⁾ using multiaperture accel-decel extraction and a Cockcroft-Walton accelerator high gradient column for an r.f. linac source.

2. The One-Ampere Cesium Source

A schematic diagram of the Cs⁺¹ beam experiment is shown in Fig. 1. Neutral Cs atoms, generated either by heating metallic Cs or a (CsCl + Ca) mixture, are sprayed onto a hot iridium plate (anode) of 30 cm dia. which is at a temperature of 1200°K-1400°K. The ionization potential of Cs (3.9V) is smaller than the work function of iridium so that most of the Cs atoms are adsorbed on the anode surface as ions. The supply rate of Cs atoms is determined by the oven temperature and is designed in such a way that there is 1/3 of a monolayer (1mC) of Cs accumulated on the anode when the extraction voltage pulse is applied to it. The Cs⁺¹ ion emission rate is determined by the temperature and coverage of the iridium hot plate and is designed to be about 5 times the space charge limited current. In this space-charge limited operation the beam emission is uniform over the surface independent of the non-uniformities of the temperature of the anode and the neutral Cs flux.

The space-charge limited current is 1A for the extraction voltage of 500 kV which was applied to the anode. Emission-limited operation occurred when the anode temperature was below 1100°K in which case the Cs⁺¹ current was independent of the applied voltage pulse and depended only upon the anode temperature.

*This work was supported by the Offices of Laser Fusion and of High Energy and Nuclear Physics of the Dept. of Energy.

Cs depletion was observed when the anode temperature was high and the neutral Cs supply was low. In this case all the available Cs ions were used up during the earlier part of the voltage pulse. The space-charge-limited condition was recovered when the oven temperature was increased in this case.

Beam neutralization could increase the current above the classical space charge limit. Our current measurement is not yet accurate enough to establish this because of the undetermined secondary electron correction. Although the secondary electron effect was measured to be small in our earlier Cs test stand experiment, we are building improved diagnostics to delineate the phenomenon.

Time-of-flight measurements, as shown in Figure 2, proved that virtually all of the beam was composed of Cs^{+1} ions. The beam also had orders of magnitude lower intrinsic neutral background pressure compared to any electron-bombardment ionization source. This is as expected since the Saha-Langmuir equation shows that more than 99% of the incident Cs atoms are ionized. The ion beam has a very low thermal velocity equal to the temperature of the anode (0.1 eV). It is thus very bright. Normalized emittance based on the thermal spread is calculated to be $\frac{\Delta y}{y} = 0.006$ cm-mrad. The final beam emittance will be determined by non-source-originated mechanisms such as lens aberrations and scattering by grids.

The source is now operating at a few μC capacity but it can be easily scaled up by increasing the extraction voltage (up to 1 MV) and the area of

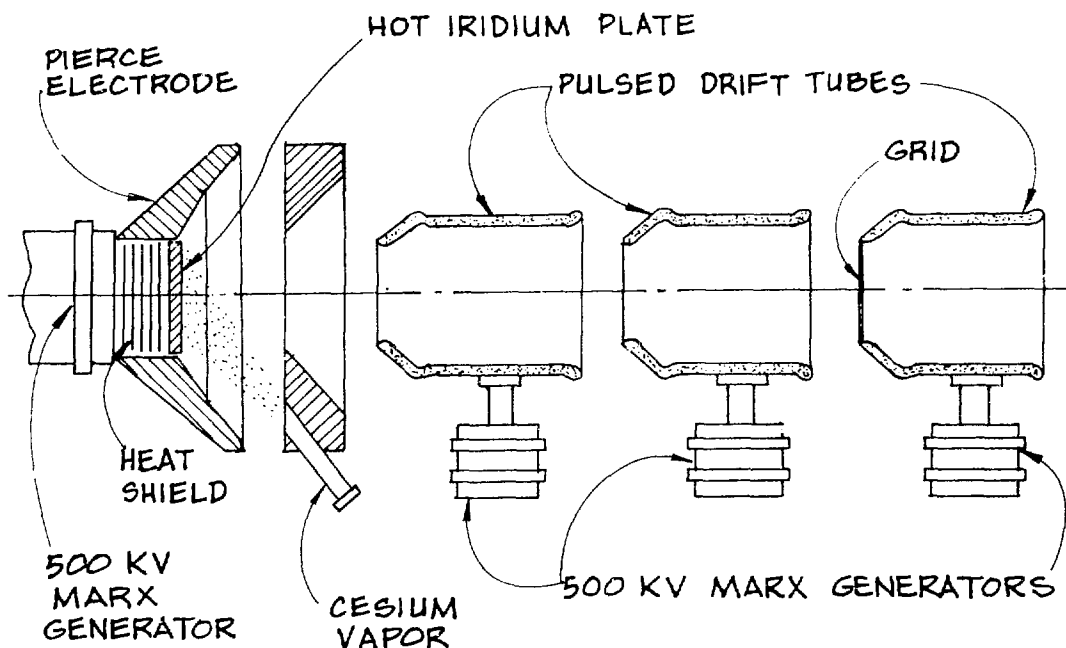


Fig. 1: Schematic diagram of the Cs^{+1} beam experiment
(Drift tube lengths not to scale)

the anode. (The contact ionization source is also applicable to uranium.⁴) Since the uranium ionization potential, approximately 6.3 volts, is higher than the work function of any refractory material, the anode needs to be oxidized or flouridated to obtain a higher work function.) The extracted Cs⁺¹ beam is focused by Pierce electrodes⁵) (Fig. 3) and will be further accelerated by a three-section pulsed drift-tube, which is being assembled at the present time. The beam will gain an increment of 500 keV per stage and reach 2 MeV at the end of the drift tubes. Other experiments under consideration are: (1) an addition of accelerating stages using induction linac cavities, and (2) a strong-focusing transport experiment.

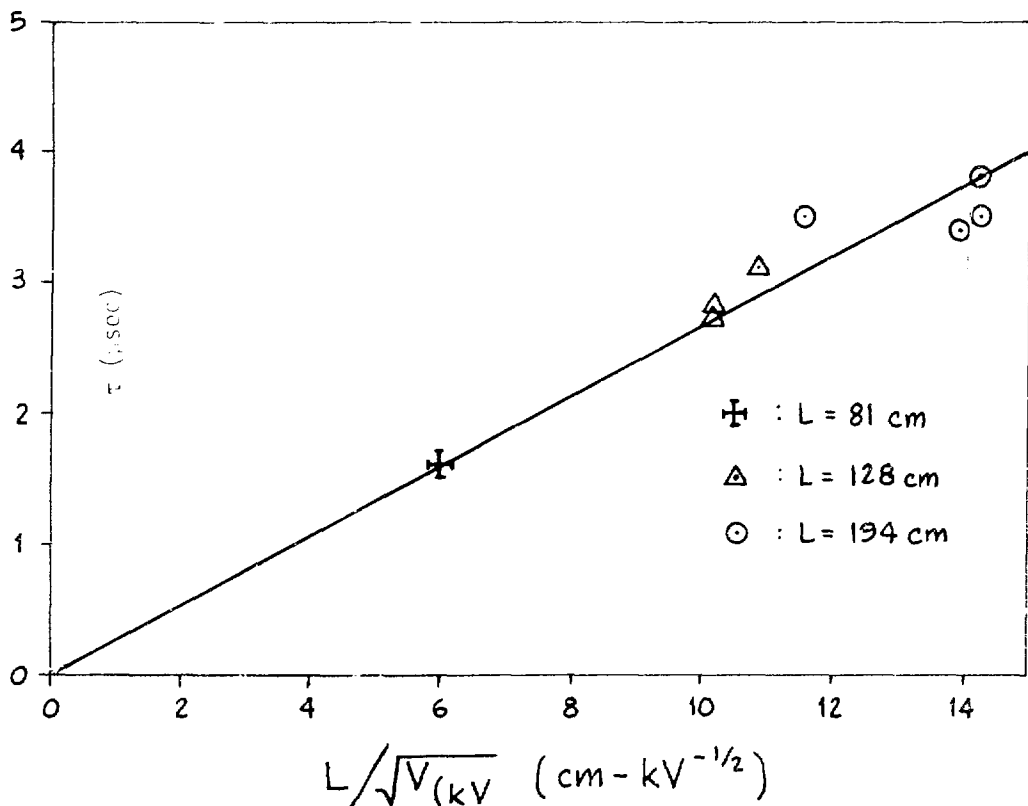


Fig. 2: Time of flight measurements of Cs⁺¹ beam. Time was measured from the end of the voltage pulse and the end of the current pulse. L_s are the distances of the drift space.

XBL 7810-12076

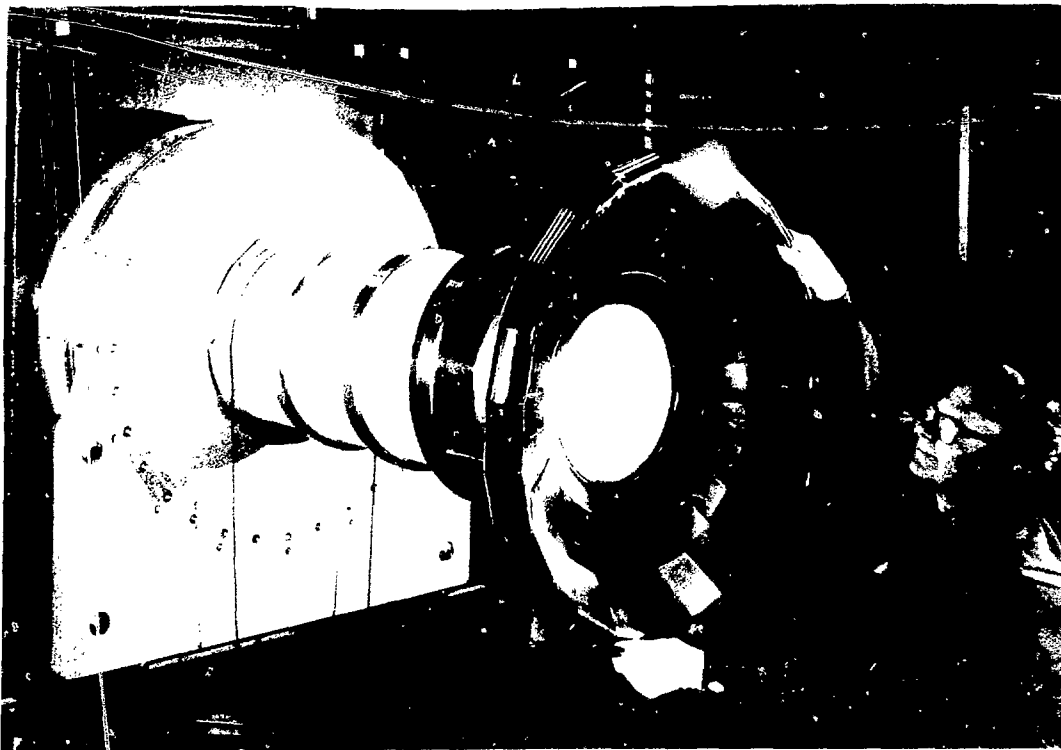


Fig. 3: A photograph showing the iridium hot plate, the Pierce electrode, and insulator column of the Cs^{+1} contact ionization source.

3. The 60 mA Xe^{+1} Source

The Xe^{+1} multiaperture source has been described in Ref. 2. The present source configuration utilizes an array of 13 holes each 4 mm in diameter symmetrically arranged within a 25 mm diameter circle. Development of this source was carried out in the Bevatron 20 kilovolt test stand.

A beam of 40 mA at 20 kV was transported one meter through a quadrupole triplet and measured with a biased Faraday cup. The measured beam diameter was 38 mm and the emittance was $\epsilon_n = \epsilon_t = 0.03 \text{ cm}^2 \text{ mrad}$. A 50-degree magnetic analysis showed the beam to contain 90% Xe^{+1} charge state.

This source was then installed in the 750 kilovolt Cockcroft-Walton accelerator. The 20 kV Xe^{+1} beam was transported one meter through two magnetic quadrupole triplets and accelerated to 500 kilovolts through the high gradient column.

A beam of 60 mA was measured with an electrically biased Faraday cup. This cup is also provided with a transverse magnetic field. The observed beam diameter was 38 mm.

The plasma arc was operated at 30 V and 50 A and a pulse length of 500 μ sec. These conditions are the same as on the 20 kilovolt test stand which yielded 90% Xe^{+1} .

A typical beam current pulse is shown in Figure 4.

Our computer calculations show that the two quadrupole triplets can only transport about 1 mA of un-neutralized Xe^{+1} . This implies that the initial beam is more than 98% neutralized.

Measurements of emittance and a magnet analysis of the beam are in progress. Following this the beam energy will be increased to 750 kV.

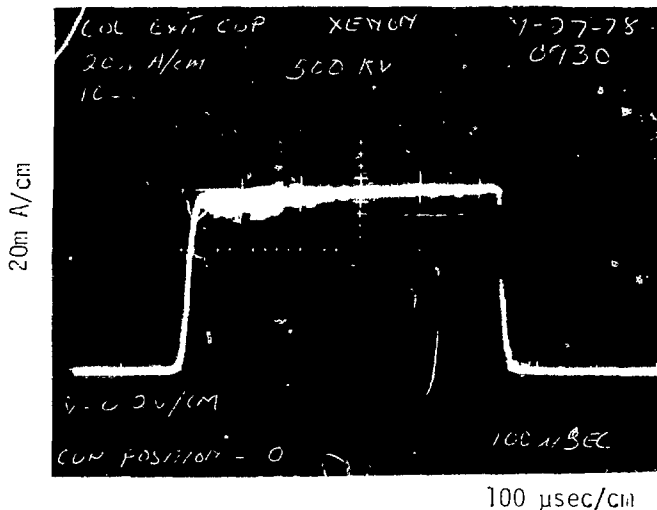


Fig. 4: 500 kV Xe^{+1} beam current vs. time

References

1. Proceedings of the Heavy Ion Fusion Workshop, Brookhaven National Laboratory Report 50769 (1977), p. 88.
2. Reference 1, page 91.
3. J. B. Taylor and I. Langmuir, Phys, Rev. 44. 423 (1933).
4. M. Hashmi, A. J. Van der Houven van Oordt, Conference on U Isotope Separation, London, March 5-7 (1975).
5. Designed by W. Herrmannsfeldt, SLAC.